A mechanistic assessment of the wet air oxidation activity of MnCeO$_x$ catalyst toward toxic and refractory organic pollutants

Francesco Arena [a,b,*], Cristina Italiano [a], Giovanni Drago Ferrante [a], Giuseppe Trunfio [a], Lorenzo Spadaro [a,b]

[a] Dipartimento di Ingegneria Elettronica, Chimica e Ingegneria Industriale, Università degli Studi di Messina, Viale F. Stagno D'Alcontres 31, I-98166 Messina, Italy
[b] Istituto CNR-ITAE "Nicola Giordano", Salita S. Lucia 5, I-98126 S. Lucia, Messina, Italy

ABSTRACT

The reactivity pattern of a *model* MnCeO$_x$ catalyst (Mn$_{at}$:Ce$_{at}$, 1) in the wet air oxidation (CWAO) of toxic (phenol) and refractory (acetic, oxalic and formic acids) organic pollutants has been probed, using a stirred batch reactor with continuous oxygen feeding (P_{O_2}, 0.9 MPa). In the range of 110–150 °C the MnCeO$_x$ catalyst (w_{cat}/w_{sub}, 5) shows high abatement and mineralization efficiency toward all the substrates. Parallel trends of substrate and total organic carbon (TOC) conversion prove that *adsorption* is the primary reaction step, while slower mineralization rates signal that *surface oxidation* is rate determining step (r.d.s.). Activity data in the pH range of 3–10 and straight relationships between conversion and dissociation constant (K_a) signal that acids adsorption is driven by electrostatic interactions with acid sites ($E_{Ads} \approx 80$ kJ/mol), while a low energetic barrier ($E_{Ads} \approx 16$ kJ/mol) discloses the physical nature of phenol adsorption. A kinetic analysis of conversion-selectivity data, based on a *dual-site* Langmuir–Hinshelwood (L–H) mechanism, sheds light into the CWAO pattern of MnCeO$_x$ catalyst toward different classes of organic pollutants.

© 2013 Elsevier B.V. All rights reserved.

1. Introduction

Uncontrolled demographic development and continuously rising standard of living determine increasing demand of essential goods from both agriculture and industry with consequent over-consumption of raw materials, depletion of water resources and huge releases to the environment. Cause of damages to ecological systems and depreciation of natural assets, this development model is modifying the natural equilibrium of Earth with severe consequences for the future of next generations. Most of all, fresh-water shortage due to huge agricultural and industrial needs, already accounting for more than 90% of current consumptions, increasing contamination of water bodies and climate changes is, in perspective, a problem of major concern [1]. This imposes new water-management policies for a proper balance of consumptions and releases, mostly by systematic implementation of recycling and reutilization procedures [2], deserving novel technical solutions to the challenging issue of industrial wastewaters purification [3–7].

Although the catalytic wet air oxidation (CWAO) represents the most adequate option for the abatement of medium–high loads of refractory and/or toxic organic pollutants [7], replacement of noble-metal catalysts with cheap, robust and active oxide systems is still the main drawback for a definitive market deployment [3–6]. Recent studies showed that conventional co-precipitated MnCeO$_x$ catalysts join higher decontamination efficiency and resistance to deactivation by *fouling* than noble-metal systems in the CWAO of phenol [8]. In spite of this, comparatively slow mineralization rates lead to an incipient formation of C1-C2 acids, with minor total organic carbon (TOC) releases during reaction time [8–10]. Constituting the residual TOC fraction of CWAO process [8–16], indeed, the mineralization of such refractory species generally requires much more severe operating conditions than heavier substrates [17–21]. Instances of high toxicity and low degradability for the conventional biological treatment systems, respectively, phenol and organic acids derivatives are also common pollutants of many industrial processes [3–5].

Therefore, this work is aimed at providing a comparative assessment of the CWAO reactivity pattern of phenol and C1-C2 (acetic, oxalic and formic) acids on a *model* MnCeO$_x$ catalyst. Catalytic data of substrates with different chemical characteristics in wide range of temperature (110–150 °C) and pH (3–10) highlight some peculiar mechanistic aspects of the CWAO of organic pollutants with different molecular weight, structure and polarity.

* Corresponding author at: Dipartimento di Ingegneria Elettronica, Chimica e Ingegneria Industriale, Università degli Studi di Messina, Italy.
Tel.: +39 090 3931346; fax: +39 090391518.
E-mail address: Francesco.Arena@unime.it (F. Arena).

Catalyst	Mn loading		SA (m^2/g)	PV (cm^3/g)	APD (nm)
	Mn$_{at}$/Ce$_{at}$	(wt%)			
MnCeO$_x$	1.0	21.4	171	0.47	20

2. Experimental

2.1. Materials

The main physico-chemical properties of the *model* MnCeO$_x$ catalyst (Mn$_{at}$/Ce$_{at}$, 1), obtained via the redox-precipitation route [14,15,22,23], are summarized in Table 1.

2.2. Methods

Wet air oxidation tests at 110–150 °C and a total pressure of 1.1–1.4 MPa (P_{O_2}, 0.9 MPa) were carried out in a PTF-lined autoclave (0.25 L), equipped with a magnetically driven impeller (≈800 rpm). The reactor was loaded with an aqueous suspension (0.15 L) of the catalyst (5 g/L) and fed with a continuous O$_2$ flow at the rate of 0.1 *stp* L min^{-1}. After reaching the reaction temperature, a concentrated substrate solution was injected (*t*, 0) into the reactor by a pressurized loop to give an initial concentration of 1 g/L ($R = w_{cat}/w_{sub}$, 5), unless otherwise specified.

Using finely powdered catalyst (d_p, 5–10 μ), mass-transfer resistances on both phenol conversion and CO$_2$ production rates for *pseudo 1st-order* kinetics are negligible, according to the Weisz–Prater criterion ($N_{W–P} < 0.15$) [8,14]

$$N_{W–P} = \frac{r_{app} \cdot \rho_p \cdot (d_p/2)^2}{D_{eff} \cdot C_S} \leq 0.03. \qquad (1)$$

where the total resistance ($1/D_{eff}$) is calculated as the contribution of external ($1/D_L$) and internal ($1/D_{pore}$) mass-transfer resistances for phenol and oxygen, respectively

$$\frac{1}{D_{eff}} = \frac{1}{D_L} + \frac{1}{D_{pore}}, \qquad (2)$$

while C_S is the concentration of phenol ($\approx 10^{-2}$ mol L^{-1}) or oxygen in the solution. According to minor variations (10–15%) of the Henry constant of the oxygen/water system in the range of 110–150 °C [6] and a large excess of continuous supply (F_{O_2}, 0.25 mol/h), the oxygen concentration in the solution can be assumed virtually constant, being comprised between 6×10^{-3} (100 °C) and 7×10^{-3} (150 °C) mol L^{-1}. In addition, the absence of diffusional resistances on the reaction kinetics was experimentally confirmed by unchanging conversion and mineralization rates recorded further to a fivefold increase of catalyst (25 g/L) and substrate (5 g/L) load (w_{cat}/w_{Phenol}, 5) [8].

The reacting solution was periodically analyzed in terms of pH; substrate and intermediates concentration, by HPLC (UVD170U, Dionex) equipped with a C6-Phenyl 110A column, and TOC, by a combustion-nondispersive IR analyzer (TOC-VCSN, Shimadzu). The CO$_2$ selectivity was also probed by gravimetric analysis of the precipitated BaCO$_3$, formed by bubbling the outlet reactor stream into a saturated Ba(OH)$_2$ solution, kept at 25 °C under stirring [8,9,14–16]. The Mn leaching was checked by Atomic Absorption Spectrometry (Analyst 200-Perkin Elmer) analysis of the reacting solution, resulting always negligible (<1 ppm).

Thermogravimetric (TGA–DSC) analysis of the "used" MnCeO$_x$ catalyst samples (≈5 mg) in the range of 20–400 °C were performed using a Simultaneous Thermal Analysis (STA 409C, NETZSCH), operating in air with a heating rate of 10 °C/min and an accuracy of ±0.01 mg. The used catalyst samples were recovered by filtration, washed with hot distilled water, and further dried in air at 100 °C before measurements.

3. Results and discussion

3.1. Wet air oxidation pattern of phenol and C1-C2 acids (blank tests)

To highlight the wet air oxidation (WAO) reactivity pattern of the studied substrates, preliminary *blank tests* in absence of catalyst at the highest reaction temperature were carried out (results not shown for the sake of brevity) [9]. An absolute lack of conversion during 6 h of reaction time confirms the poor WAO reactivity of acetic and formic acids at 150 °C [3–6,17,18], while despite final conversion and CO$_2$ selectivity values of ca. 60% and 10% respectively, phenol conversion and mineralization rates are negligible compared to those of MnCeO$_x$ catalyst [9]. At last, oxalic acid is the only substrate undergoing a complete conversion after 6 h, with a simultaneous CO$_2$ production corresponding to a constant selectivity of ≈50% throughout reaction time.
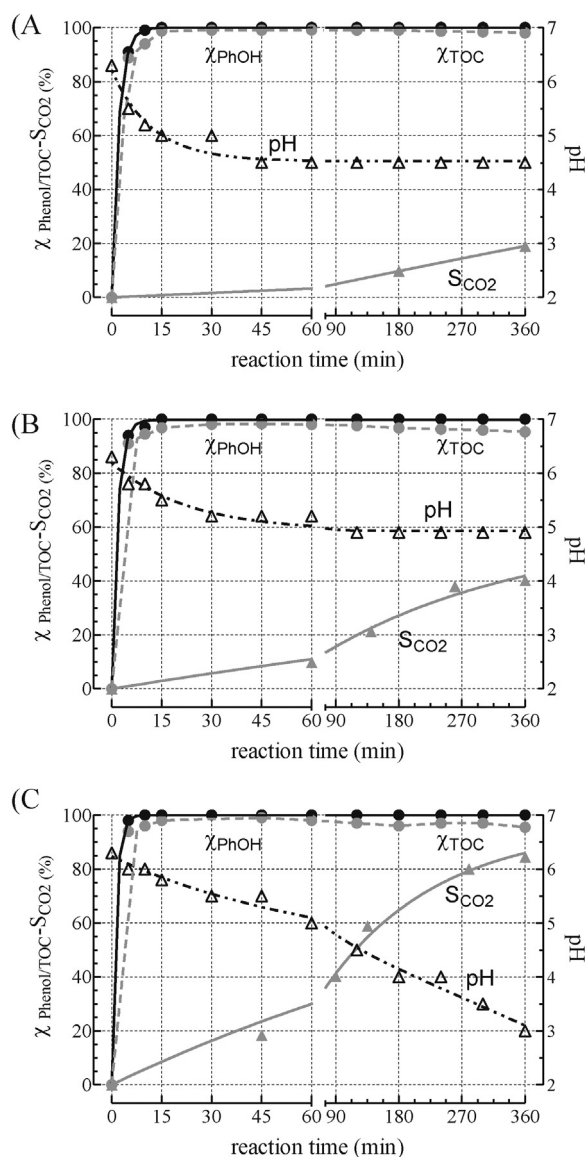

Fig. 1. CWAO reactivity pattern of phenol at 110 (A), 130 (B) and 150 °C (C). Phenol and TOC conversion, pH and CO$_2$ selectivity vs. reaction time.
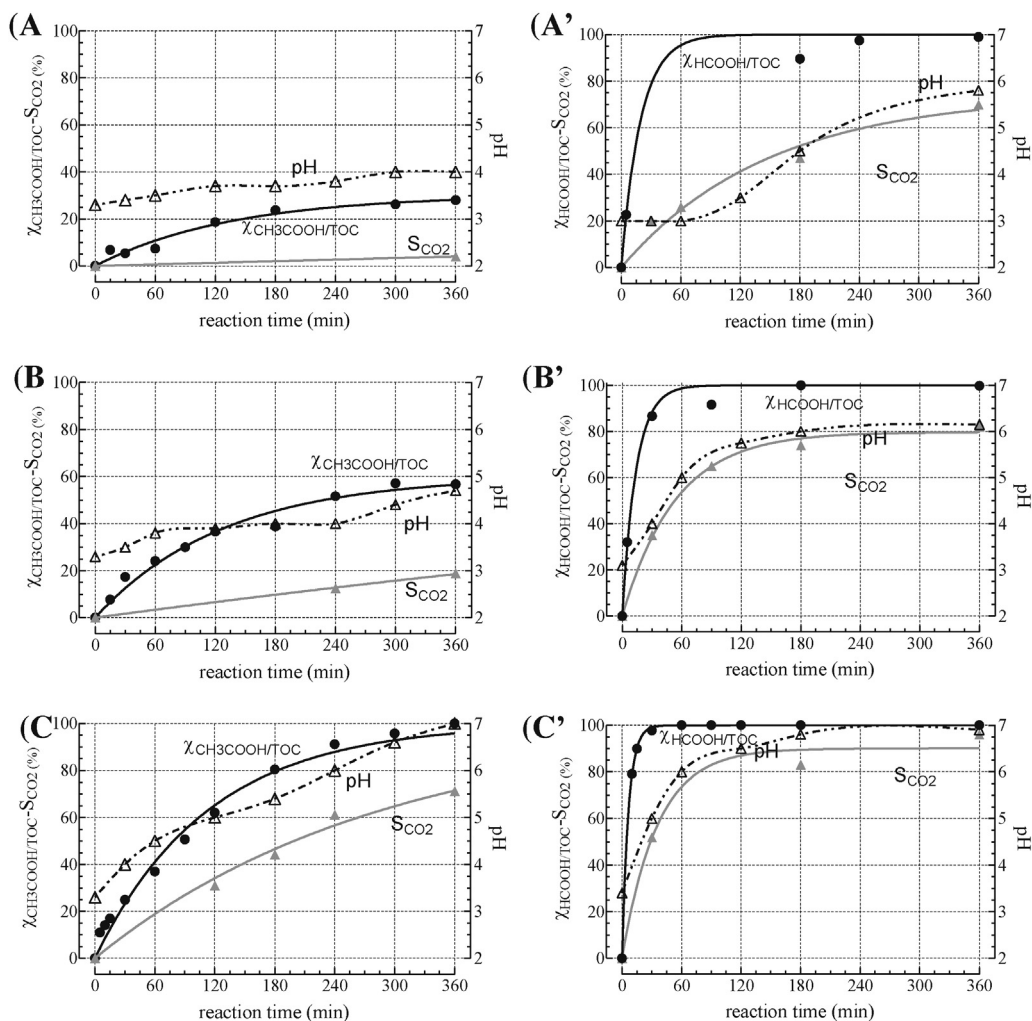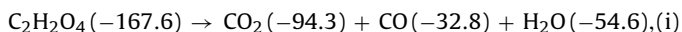
Fig. 2. CWAO reactivity pattern of acetic (A–C) and formic (A'–C') acids at 110 (A and A'), 130 (B and B') and 150 °C (C and C'). Substrate/TOC conversion, pH and CO$_2$ selectivity vs. reaction time.

According to the free energy of formation ($\Delta G°$, kcal/mol) of substrate and products

$$C_2H_2O_4 (-167.6) \rightarrow CO_2 (-94.3) + CO (-32.8) + H_2O (-54.6), \text{(i)}$$

the high WAO reactivity of oxalic acid is attributable to the high stability of products favoring the decomposition reaction (i), as confirmed by GC analysis of the reactor stream, showing an equimolar formation of CO and CO$_2$. This accounts for a negligible lifetime under CWAO conditions (w_{cat}/w_{Phenol}, 5) in the range of 110–150 °C and, then, oxalic acid was not longer considered henceforth.

3.2. CWAO pattern of phenol and C1-C2 acids: effect of temperature

The CWAO data of phenol in the range of 110–150 °C (w_{cat}/w_{Phenol}, 5) are shown in Fig. 1, in terms of substrate and total organic carbon (TOC) conversion, pH and CO$_2$ selectivity during 6 h of reaction time. The MnCeO$_x$ catalyst enables a simultaneous removal of phenol and TOC at any temperature, in a time ranging between 30 (110 °C) and 10 min (150 °C); thereafter, phenol is not longer detected, while a slight though progressive rise of TOC is observed at $T \geq 130$ °C. The pH decreases from 6.0–6.5 to values of 5.0–4.0 at 110–130 °C, reaching a minimum of ca. 3.5 at 150 °C, due always to the prevalent accumulation of acetic acid [8–10,12–16], which explains the aforesaid TOC "release" (Fig. 1C). The CO$_2$

selectivity grows regularly with time and temperature to final values ranging from 20% to 90% in the range of 110–150 °C, respectively.

The MnCeO$_x$ catalyst shows to be active also in the CWAO of acidic compounds (Fig. 2), though conversion and mineralization rates depend on the nature of the substrate. Indeed, lower conversion rates and a CO$_2$ selectivity rising from 10% to 70% in the range of 110–150 °C (Fig. 2A–C) confirm that acetic acid is the most refractory pollutant, also in presence of MnCeO$_x$ catalyst. A complete abatement is recorded after 6 h only at 150 °C (Fig. 2C), while at 110 and 130 °C the final conversion is equal to 30% (Fig. 2A) and 60% (Fig. 2B), respectively. The higher reactivity of formic acid is evident from the complete conversion recorded at any temperature, in a time shortening from 270 to 60 min, and final CO$_2$ selectivity values going from 40% to 80% in the range of 110–150 °C (Fig. 2A'–C'), respectively. Moreover, contrarily to phenol (Fig. 1), the ongoing proton consumption by the relative *mineralization* reactions

$$HCOO^- + H^+ + 1/2O_2 \rightarrow CO_2 + H_2O \tag{ii}$$

$$CH_3COO^- + H^+ + 2O_2 \rightarrow 2CO_2 + 2H_2O \tag{iii}$$
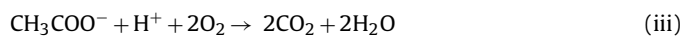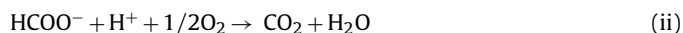
reflects in a progressive rise of pH from acidic to neutral values (Fig. 2), somewhat hindering both adsorption and mineralization processes at high extent of substrate mineralization (see *infra*). Then, the CWAO data of a mixture of phenol (R, 5), formic (R, 30) and
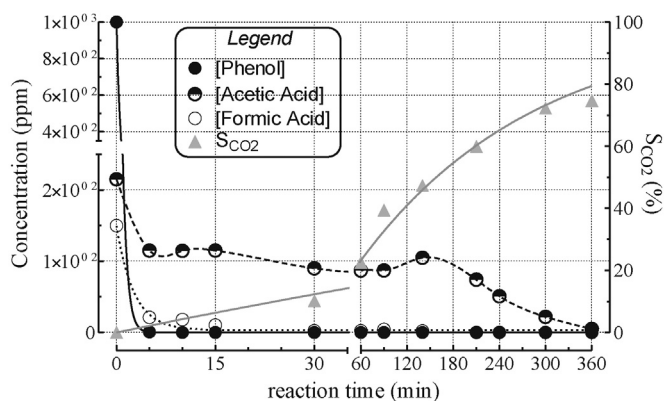
Fig. 3. CWAO reactivity pattern at 150 °C of a mixture of phenol (R, 5), acetic (R, 20) and formic acids (R, 30). Substrates conversion and CO_2 selectivity vs. reaction time.

acetic acids ($R = 20$) at 150 °C are shown in Fig. 3. A fast (10–15 min) and complete conversion of phenol and formic acid substantiates the CWAO efficiency of MnCeO$_x$ catalyst also toward a mixture of the studied substrates, though acetic acid concentration lowers by ca. one-half during the first 30 min, depicting a plateau ($\approx$100 ppm) that slowly disappears during the last 3 h of reaction time. This peculiar trend reflects the fact that the ongoing conversion of acetic acid is counterbalanced by the release of the same species, coming from the uncomplete oxidation of phenol [8–10,14]. Therefore, the above results signal that the CWAO performance of MnCeO$_x$ catalyst toward phenol and C1-C2 acids is the result of its reactivity pattern toward each single compound, also in terms of the final CO_2 selectivity value (80%).

3.3. Mechanistic–kinetic analysis

Although conversion rates systematically higher than mineralization ones denote the transient regime of CWAO tests, from a mechanistic point of view the above data signal the occurrence of a typical heterogeneous Langmuir–Hinshelwood (L–H) reaction path [8,9,12–15]. In fact, surface adsorption as first reaction step accounts for the faster and parallel substrate and TOC conversion, while a slower mineralization of adsorbed species to CO_2 suggests that surface oxidation is the rate determining step (r.d.s.) of the CWAO process [8,9,12–15]. Formation and release of light reaction intermediates and C-deposits build up (e.g., catalyst fouling) are undesired side processes of the mineralization step, accounting for selectivity and catalyst stability, respectively [8,9,14]. This is substantiated by the dynamics of the catalyst surface during CWAO processes, probed by the weight changes of representative "used" catalyst samples recorded by TGA–DSC measurements. The results in Fig. 4A show that the sample used at 150 °C for 20 min features a weight loss of 16–17%, coupled to a very intense exo-signal (Fig. 4A), accounting for the combustion of an amount of adsorbed phenol which corresponds to the initial catalyst-to-phenol weight ratio (5/1). This proves that a very fast adsorption leads to a complete phenol/TOC removal (e.g., conversion) in less than 15 min (Fig. 1C). Thereafter, a parallel lessening of weight loss and DSC peak (Fig. 4A) accounts for the progressive mineralization of the adsorbed substrate, in a good agreement with the time trend of CO_2 selectivity (Fig. 1C). Likewise, weight losses decreasing from 15% to 3% (Fig. 4B) match with final CO_2 selectivity values increasing from 20% to 90% in the range of 110–150 °C (Fig. 1A–C).

Parallel trends of substrate and TOC conversion, a systematic gap in C-mass balance, according to different TOC conversion and CO_2 selectivity levels, and buildup of considerable amounts of C-containing species on catalyst samples (Table 2) suggest that the CWAO of acids proceeds via the same sequence of reaction steps
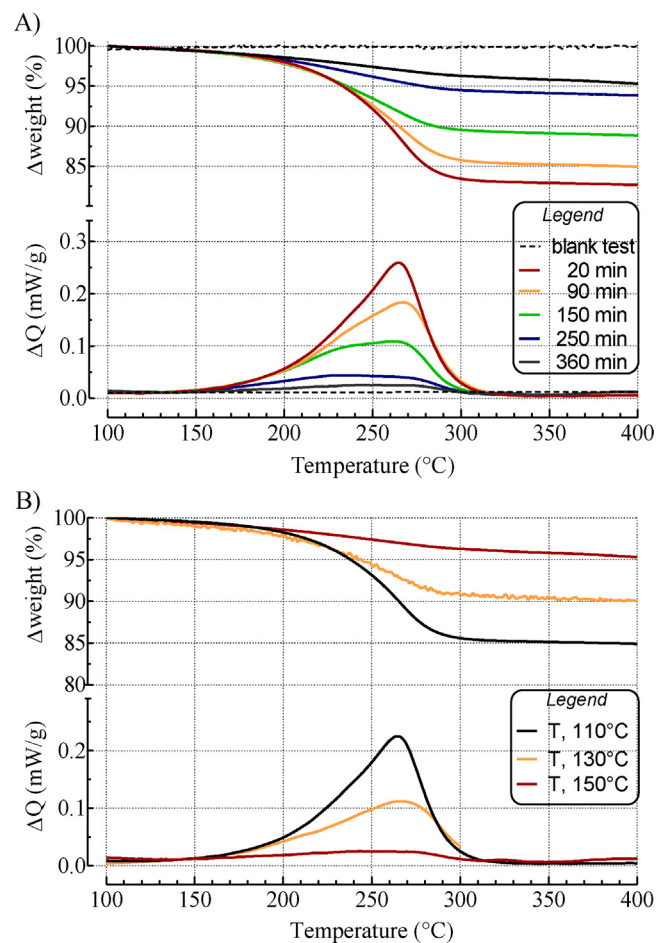

Fig. 4. TGA–DSC data of the "used" catalyst samples in the CWAO of phenol: (A) at 150 °C after different reaction time and (B) at different temperature (110–150 °C) after 6 h of reaction time.

(adsorption → oxidation → desorption), typical of the L–H mechanism. Accordingly, the rate of conversion due to non-dissociative adsorption is described by a 1st-order law on substrate concentration C_{Sub} (mol L^{-1})

$$\text{rate}_{Conv} = \text{rate}_{Ads} = -\frac{dC_{Sub}}{dt} = k_{Conv} \cdot C_{Sub}, \tag{3a}$$

though very large extents ($\gg$10%) of conversion (Figs. 1 and 2) deserve the integral forms of Eq. (3a)

$$\frac{C_{Sub}}{C_{Sub,in}} = e^{-k_{Conv} \cdot t} \Rightarrow -\ln\left(\frac{C_{Sub}}{C_{Sub,in}}\right) = k_{Conv} \cdot t \tag{3b}$$

for calculation of k_{Conv} values by the fitting of experimental data, as shown in Fig. 5A–A''. In turn, these were transformed in the catalytic 1st-order kinetic constants (L g$_{cat}^{-1}$ h^{-1}) of adsorption ($k_{Ads} = [k_{Conv}/C_{cat}]$), summarized in Table 3.

Table 2
Weight loss of the used catalyst in the CWAO of acetic and formic acids (110–150 °C).

Substrate	T (°C)	Δweight (%)	C_{Ads} (mol$_{Sub}$ g$_{cat}^{-1}$)
Acetic acid	110	−8.0	1.5E−3
	130	−8.0	1.5E−3
	150	−5.5	1.0E−3
Formic acid	110	−5.0	1.1E−3
	130	−4.0	8.5E−4
	150	−2.0	4.2E−4

The highest conversion rates of phenol mirror k_{Ads} values between 5.8 and 9.4 $L\,g_{cat}^{-1}\,h^{-1}$ in the range of 110–150 °C, accounting for a very low (E_{Ads}, 16 kJ/mol) energetic barrier of the adsorption process (Table 3). In this respect, lack of diffusional resistances (see Section 2) and boiling point ($\approx$182 °C) higher than reaction temperature lead to infer that phenol adsorption could be driven by physical condensation in the porous structure of the catalyst. On the other hand, the lower "reactivity" of acids reflects in systematically smaller k_{Ads} values, which are yet much more dependent on temperature (Table 3). Namely, formic acid shows k_{Ads} values between 5 and 10 times smaller in the range of 110–150 °C, while the poorest reactivity of acetic acid is substantiated by k_{Ads} values lower by 2–3 orders of magnitude than phenol (Table 3). Despite of this, a similar growth in the range of 110–150 °C mirrors comparable higher values of the energetic barrier (E_{Ads}, 75–85 kJ/mol) of adsorption for acetic and formic acids (Table 3), diagnostic of "true" chemical interactions between substrate and catalyst. This depends on the chemical characteristics of the substrates as, at variance of the aromatic and almost apolar phenol molecule, the polarity of the carboxylic group likely triggers "specific" (i.e., electrostatic) interactions between the conjugated base ($RCOO^-$) and surface acid sites (α^+). This interaction pattern surmises some influence of the acid dissociation constant (K_a) on the adsorption rate, as it determines the concentration of negatively charged carboxylate species ($C_{RCOO^-} = K_a \cdot C_{RCOOH^-}/C_{H^+}$). However, due to the unfeasibility of getting K_a values in the range of 110–150 °C, the adsorption constants (k_{Ads}) of the three substrates are compared with the relative K_a values at 25 °C [24] in Fig. 6A. Despite the considered K_a values refer to a temperature much lower than that of reaction, direct relationships with a constant slope of $\approx$1 (1.1–1.2) likely indicate a linear dependence of k_{Ads} on K_a for the two acidic substrates

$$k_{Ads}(L\,g_{cat}^{-1}\,h^{-1}) = k_{Cat}(L^2\,mol^{-1}\,g_{cat}^{-1}\,h^{-1}) \cdot K_a(mol\,L^{-1}), \quad (4)$$

documenting that the adsorption rate of acidic compounds depends on a thermodynamic constant (K_a), specific of the substrate, and a 2nd-order kinetic constant (k_{Cat}), typical of the catalyst and relative to the following displacement reaction at the catalyst surface:

$$RCOOH + \alpha\text{-}OH \leftrightharpoons RCOO\text{-}\alpha + H_2O. \quad (iv)$$
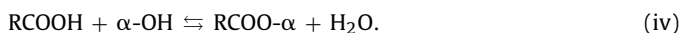
Indeed, rewriting Eq. (3a) in terms of the kinetic constant and catalyst concentration ($k_{Cat} \cdot C_{Cat}$)

$$rate_{Ads} = (k_{Cat} \cdot C_{Cat}) \cdot K_a \cdot C_{Sub}, \quad (3c)$$

and considering that

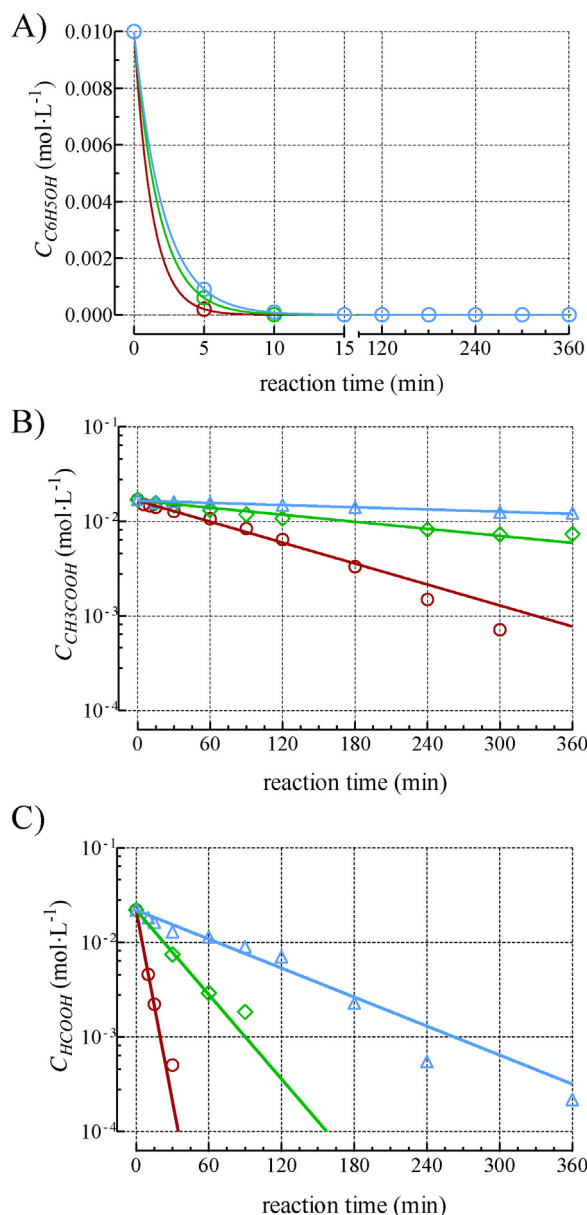$$K_a \cdot C_{Sub} = C_{RCOO^-} \cdot C_{H^+}, \quad (5)$$

Fig. 5. Fitting of conversion data in the range of 110–150 °C of phenol (A), acetic (B) and formic (C) acids by 1st-order model Eqs. (3b), (4c) and (4d).

Table 3
1st-order kinetic constants of substrate conversion and pseudo 1st-order constants of mineralization of the various substrates in the range of 110–150 °C.

Substrate	T (°C)	Conversion (adsorption)			Mineralization			
		$r^2\ k_{Conv}$[a] (min^{-1})	k_{Ads} (L g^{-1} h^{-1})	E_{Ads} (kJ/mol)	$r^2\ k_{Min}$[b] (min^{-1})	k_{CO_2} (L g^{-1} h^{-1})	E_{CO_2} (kJ/mol)	k_{CO_2}/k_{Ads}
Phenol	110	1.000 4.8E−1	5.8E+0		1.000 5.8E−4	4.2E−2		0.01
	130	1.000 5.6E−1	6.7E+0	16 ± 4	0.994 1.5E−3	1.1E−1	75 ± 9	0.02
	150	1.000 7.8E−1	9.4E+0		0.999 5.4E−3	3.9E−1		0.04
Acetic acid	110	0.975 8.9E−4	1.1E−2		0.992 3.2E−4	7.6E−3		0.69
	130	0.955 2.9E−3	3.5E−2	76 ± 1	0.986 9.6E−4	2.3E−2	84 ± 8	0.66
	150	0.990 8.5E−3	1.0E−1		0.999 3.9E−3	9.4E−2		0.94
Formic acid	110	0.965 1.2E−2	1.4E−1		0.998 5.9E−3	7.1E−2		0.51
	130	0.998 3.4E−2	4.1E−1	86 ± 11	0.997 1.9E−2	2.3E−1	79 ± 2	0.56
	150	1.000 1.5E−1	1.8E+0		0.996 6.2E−2	7.4E−1		0.41

[a] 1st-order kinetic constants of substrate conversion obtained from the fitting of experimental data by Eq. (3b).
[b] pseudo 1st-order kinetic constants of substrate mineralization obtained from the fitting of experimental conversion-selectivity data by Eqs. (6c) and (6d).
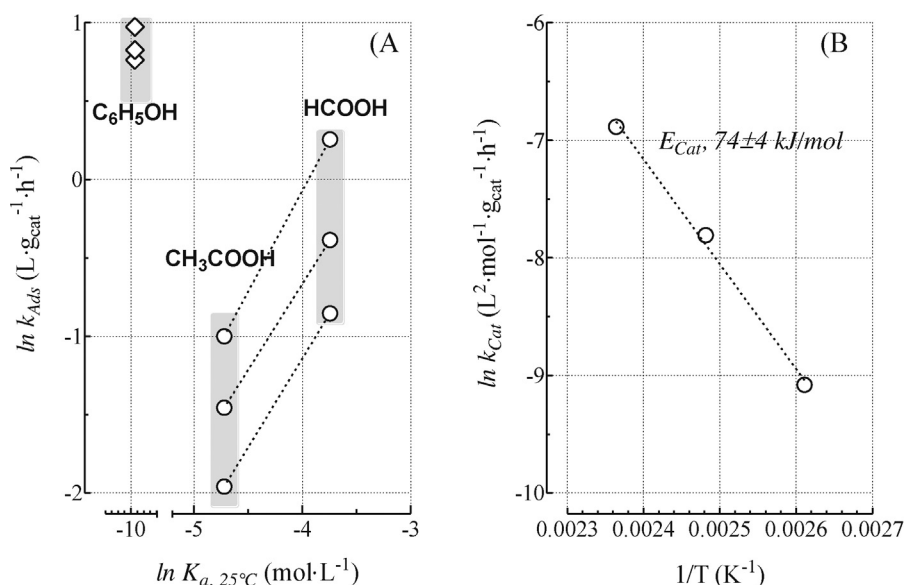
Fig. 6. (A) "log-plot" of the *pseudo 1st-order* kinetic constant of adsorption (k_{Ads}) vs. the relative acidic constant at 25 °C (K_a) of the various substrates in the range of 110–150 °C; and (B) Arrhenius plot of the catalyst 2nd-order intrinsic constant of adsorption (k_{Cat}).

the new equation

$$rate_{Ads} = (k_{Ads} \cdot C_{Cat}) \cdot C_{RCOO^-} \cdot C_{H^+} \tag{3d}$$

discloses that the rate of acids adsorption depends on the concentration of both conjugated base and protons. Showing that proton concentration is a potential kinetic term for adsorption, Eq. (3d) well accounts for the poor, if any, reactivity of organic acids generally observed at basic pH [3–5]. In fact, proton concentration has a direct influence on adsorption rate as it determines the polarization of surface hydroxyl groups

$$H^+ + \alpha\text{-OH} \leftrightarrows \alpha\text{-OH}_2{}^+ \leftrightarrows \alpha^+ + H_2O. \tag{v}$$
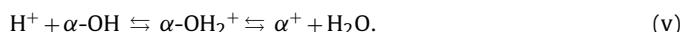
On this account, a maximum gap of 40% between extent of acid/TOC conversion and CO_2 selectivity (Fig. 2) would signal a saturation capacity of 1.5 mmol $g_{cat}{}^{-1}$ (Table 2), corresponding to a surface hydroxyl density of ca. $10^{-5}/m^2$ that, although larger, compares with the density of acid-basic sites previously found ($\approx 3 \times 10^{-6}/m^2$) by gas-phase NH_3/CO_2 TPD measurements [25]. In this respect, it can be speculated that the extensive surface hydroxylation could enhance the catalyst adsorption capacity under CWAO conditions.

Then, the k_{Cat} values in the range of 110–150 °C, obtained from the intercept values at $\ln(k_{Ads}) = 0$ (Fig. 6A) and elaborated into the Arrhenius plot in Fig. 6B, account for an activation energy of 74 ± 8 kJ/mol. This activation energy value, equal to E_{Ads} of both substrates (Table 3), confirms that the degree of dissociation controls the acids adsorption rate without affecting the mechanism and, consequently, the energetic barrier of electrostatic adsorption. Whilst no $k_{Ads} - K_a$ relationship supports the different mechanism of phenol adsorption (Fig. 6A). These findings explain the removal efficiency of MnCeO$_x$ catalyst toward both phenol and C1-C2 species (Fig. 3), while the marked effect of pH on the conversion rate of the studied substrates is evident from the comparison of CWAO data (150 °C) of phenol and acetic acid at "free" and basic (≈ 10) pH conditions, reported in Fig. 7. Phenol conversion rate is not affected by pH, according to the physical nature of the relative adsorption process, while acetic acid conversion is strongly depressed to a plateau of ca. 15%, comparing to the complete abatement recorded at acidic pH (Fig. 2C). Despite the complete dissociation of the substrate, the inhibiting effect of OH^- ions on acid adsorption depends on the negative polarization of the hydroxyl

groups which, in turn, hinder the electrostatic interaction with carboxylic species. Moreover, the negative influence of basic pH on the CWAO of acids is enhanced by the pH-dependent mineralization reaction (reaction (iii)).

In fact, beside to the lack of pH-effects also on the oxidation of phenol

$$C_6H_6O + 7O_2 \rightarrow 6CO_2 + 3H_2O, \tag{v}$$

the specificity of the CWAO pattern of the various substrates concerns also the efficiency of the mineralization process, according to the following kinetic analysis. In particular, at variance of adsorption, the mineralization process is a "surface" reaction step depending on the amount of adsorbed substrate ($C_{Sub,Ads}$, mol $g_{cat}{}^{-1}$) [8]

$$rate_{Min} = \frac{1}{n_C} \cdot \frac{dC_{CO_2}}{dt} = (k_{O_x} \cdot C_{O_2}) \cdot C_{Sub,Ads}, \tag{6a}$$

where n_C is the number of C-atoms of substrates, K_{O_x} ($L\,mol^{-1}\,min^{-1}$) is the 2nd-order constant of oxidation and C_{O_2} the oxygen concentration, respectively. Nevertheless, a nearly constant O_2 concentration in the solution (C_{O_2}, $6–7 \times 10^{-3}\,mol\,L^{-1}$) in the range of 110–150 °C [6], ensured by the continuous feed (F_{O_2}, 0.25 mol/h), allows the C_{O_2} term to be taken constant and included
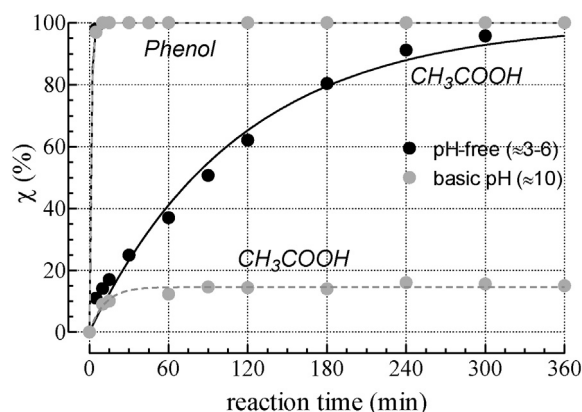

Fig. 7. Conversion pattern of phenol and acetic acid at 150 °C under "free" and basic pH (≈ 10) conditions.
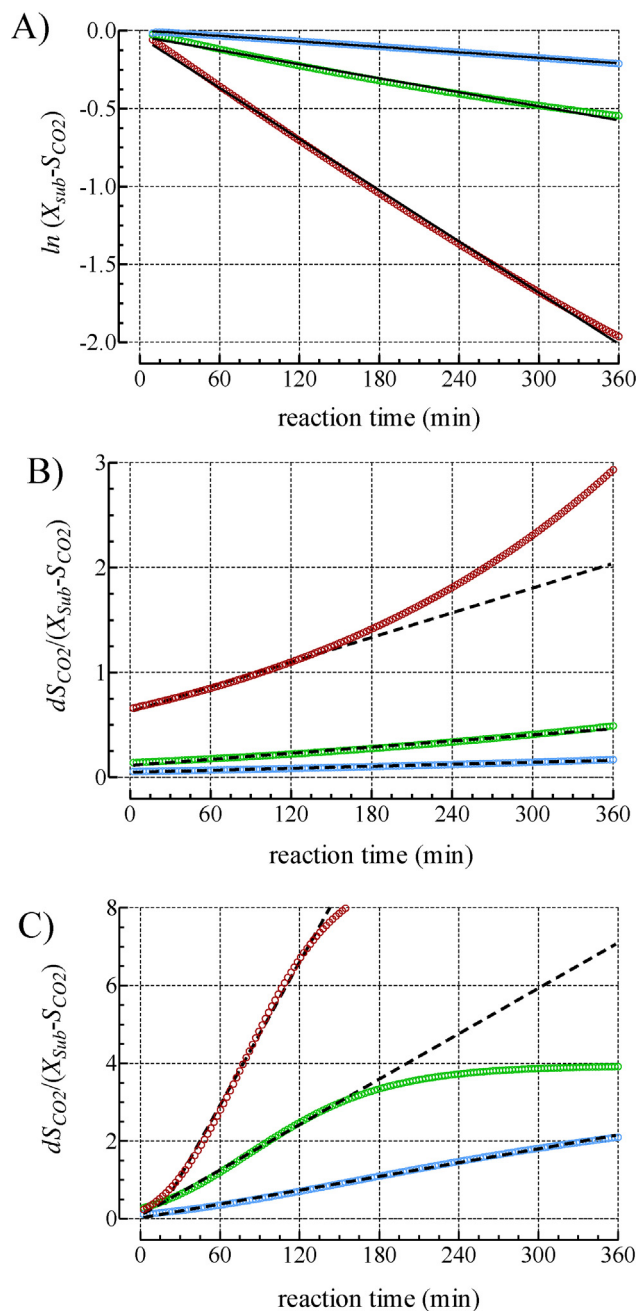
Fig. 8. Fitting of conversion-selectivity data of phenol by Eq. (6d) (A) and acetic (B) and formic acids (C) by Eq. (6c), respectively.

in a pseudo 1st-order catalytic constant ($K_{O_x} \cdot C_{O_2}$) of mineralization (k_{Min}, min^{-1}).

Then, considering the following relationship

$$C_{Sub,Ads} \cdot C_{cat} = (C_{Sub,in} - C_{Sub}) - \frac{C_{CO_2}}{n_C} = C_{Sub,in} \cdot (X_{Sub} - S_{CO_2}), \quad (7)$$

the mineralization rate (Eq. (6a)) can be written in terms of substrate conversion and C_{O_2} selectivity

$$\frac{1}{n_C} \cdot \frac{dC_{CO_2}}{dt} = k_{Min} \cdot C_{Sub,in} \cdot (X_{Sub} - S_{CO_2}) \quad (6b)$$

$$\frac{dS_{CO_2}}{(X_{Sub} - S_{CO_2})} = k_{Min} \cdot dt. \quad (6c)$$

However, if conversion is much faster than mineralization, its time dependence will be negligible ($dX_{Sub} \approx 0$), allowing Eq. (6c) to be integrated in the following straight-line function

$$-\ln\left(X_{Sub} - S_{CO_2}\right) = k_{Min} \cdot t, \quad (6d)$$

the slope of which corresponds to k_{Min}. Indeed, this results in a very accurate fit of conversion-selectivity data of phenol by Eq. (6d) (Fig. 8A) [8], while continuously changing conversion and selectivity values (Fig. 2) denote comparable rates of the conversion and mineralization processes, deserving the use of the differential Eq. (6c) for calculation of k_{Min} of acidic species (Fig. 8B and C). Then, for sake of comparison, k_{Min} were transformed into the catalytic pseudo 1st-order constant ($k_{CO_2} = [(k_{Min} \cdot n_C)/C_{Cat}]$) of CO_2 formation ($L\,g_{cat}^{-1}\,h^{-1}$), also listed in Table 3. Namely, phenol features k_{Min} values 2–3 orders of magnitude lower than k_{Conv} (Table 3), accounting for an energetic barrier (E_{CO_2}, 75 kJ/mol) considerably higher than adsorption (Table 3) and confirming that mineralization is the rate determining step (r.d.s.) of the CWAO of phenol [8,9,12–15]. In this respect, it must be emphasized that just a very effective oxygen supply allows in our case the kinetic-control of the mineralization process, whereas strongly limited mineralization rates under static O_2 atmosphere cause huge buildup of carbon deposits on the surface of unpromoted and Pt-promoted MnO_x–CeO_2 catalysts, as reported by Kouraichi et al. in the CWAO of phenol at 140 °C [26].

Although organic acids show k_{Min} values comparable to those of phenol, acetic acid confirms its higher resistance also to mineralization with k_{Min} values smaller than both phenol and formic acid (Table 3). However, k_{CO_2}/k_{Ads} ratios between 0.4–0.6 and 0.7–0.9, respectively, indicate that the CWAO of both acidic substrates proceeds with comparable rates of the adsorption and mineralization steps, while similar E_{CO_2} values (79–84 kJ/mol) equal to E_{Ads} ones disclose also comparable energetic barriers of the main reaction steps (Table 3).

Therefore, E_{CO_2} values (79 ± 5 kJ/mol) independent from the nature of the substrate suggest that the activation energy of the mineralization step depends mostly on the redox activity of the catalyst and, particularly, on its capability to generate surface electrophylic oxygen species by "Mn^{n+}–O^{m-}" electron-transfer(s), in charge of the oxidation process of adsorbed species [27].

4. Conclusions

Mechanistic and kinetic clues of the CWAO of toxic (phenol) and refractory (C1-C2 acids) organic pollutants by a *model* $MnCeO_x$ catalyst have been addressed.

$MnCeO_x$ catalyst shows a high CWAO efficiency toward phenol and C1-C2 organic acids in terms of adsorption and mineralization rates.

The CWAO of phenol proceeds via a L–H mechanism, involving *adsorption* as first reaction step and *surface oxidation* as *rate determining step* (r.d.s.), while adsorption and mineralization steps of acidic substrates proceed at comparable rate.

The removal of C1-C2 acids is driven by electrostatic adsorption on catalyst surface acid sites, while phenol adsorption is ascribable to physical condensation in the pore structure of the catalyst.

$MnCeO_x$ catalyst shows high purification efficiency toward toxic and refractory compounds, deserving potential applications in the CWAO of complex industrial wastewater streams.

List of acronyms

K_a	acid dissociation constant at 25 °C ($mol\,L^{-1}$)
k_{Conv}	1st order constant of substrate conversion (min^{-1})

k_{Min} — pseudo 1st order constant of substrate mineralization (min^{-1})

$rate_{Conv}$ — rate of substrate conversion ($mol\,L^{-1}\,h^{-1}$)

$rate_{Min}$ — rate of substrate mineralization ($mol\,L^{-1}\,h^{-1}$)

k_{Ads} — catalyst specific 1st order constant of substrate adsorption ($L\,g_{cat}^{-1}\,h^{-1}$)

k_{CO_2} — catalyst specific pseudo 1st order constant of CO_2 formation ($L\,g_{cat}^{-1}\,h^{-1}$)

k_{Cat} — catalyst specific 2nd order constant of acid adsorption ($L^2\,mol^{-1}\,g_{cat}^{-1}\,h^{-1}$)

C_{Sub} — substrate concentration ($t = t$) ($mol\,L^{-1}$)

$C_{Sub,in}$ — initial substrate concentration ($t = t_0$) ($mol\,L^{-1}$)

$C_{Sub,Ads}$ — adsorbed substrate concentration ($mol\,g_{cat}^{-1}$)

C_{Cat} — catalyst load (g/L)

X_{Sub} — substrate conversion

S_{CO_2} — CO_2 selectivity

Acknowledgement

References

[1] C. Cooney, Environmental Science and Technology 43 (2009) 3986.
[2] J. Kemsley, C&EN 28 (January) (2008) 71.
[3] G. Busca, S. Berardinelli, C. Resini, L. Arrighi, Journal of Hazardous Materials 160 (2008) 265.
[4] K.H. Kim, S.-K. Ihm, Journal of Hazardous Materials 186 (2011) 16.
[5] S.K. Bhargava, J. Tardio, J. Prasad, K. Föger, D.B. Akolekar, S.C. Grocott, Industrial and Engineering Chemistry Research 45 (2006) 1221.
[6] F. Larachi, Topics in Catalysis 33 (2005) 109.
[7] J. Hertrampf, A.H. Shadiaky, Chemical Engineering (August) (1999) 72.
[8] F. Arena, C. Italiano, L. Spadaro, Applied Catalysis B 115–116 (2012) 336.
[9] F. Arena, C. Italiano, A. Raneri, C. Saja, Applied Catalysis B 99 (2010) 321.
[10] S. Imamura, Industrial and Engineering Chemistry Research 38 (1999) 1743.
[11] S.T. Hussain, A. Sayari, F. Larachi, Journal of Catalysis 201 (2001) 153.
[12] M. Abecassis-Wolfovich, M.V. Landau, A. Brenner, M. Herskowitz, Industrial and Engineering Chemistry Research 43 (2004) 5089.
[13] M. Abecassis-Wolfovich, R. Jothiramalingam, M.V. Landau, M. Herrskowitz, B. Viswanathan, T.K. Varadarajan, Applied Catalysis B 59 (2005) 91.
[14] F. Arena, J. Negro, A. Parmaliana, L. Spadaro, G. Trunfio, Industrial and Engineering Chemistry Research 46 (2007) 6724.
[15] F. Arena, G. Trunfio, J. Negro, L. Spadaro, Applied Catalysis B 85 (2008) 40.
[16] F. Arena, R. Giovenco, T. Torre, A. Venuto, A. Parmaliana, Applied Catalysis B 45 (2003) 51.
[17] J. Barbier Jr., F. Delanoë, F. Jabouille, D. Duprez, G. Blanchard, P. Isnard, Journal of Catalysis 177 (1998) 378.
[18] J. Mikulová, S. Rossignol, J. Barbier Jr., D. Mesnard, C. Kappenstein, D. Duprez, Applied Catalysis B 72 (2007) 1.
[19] J. Mikulová, J. Barbier Jr., S. Rossignol, D. Mesnard, D. Duprez, C. Kappenstein, Journal of Catalysis 251 (2007) 172.
[20] J. Wang, W. Zhu, X. He, S. Yang, Catalysis Communications 9 (2008) 2163.
[21] J. Gaálová, J. Barbier Jr., S. Rossignol, Journal of Hazardous Materials 181 (2010) 633.
[22] F. Arena, G. Trunfio, J. Negro, B. Fazio, L. Spadaro, Chemistry of Materials 19 (2007) 2269.
[23] F. Arena, L. Spadaro, Pending Patent Appl. n. PCT/IT2012/000172 (2012).
[24] I.M. Kolthoff, E.B. Sandell, E.J. Mehan, S. Bruckenstein, Quantitative Analytical Chemistry, vol. 1, Piccin Edition, Padua, Italy, 1973.
[25] C. Cannilla, G. Bonura, E. Rombi, F. Arena, F. Frusteri, Applied Catalysis A 382 (2010) 158.
[26] R. Kouraichi, J.J. Delgado, J.D. López-Castro, M. Stitou, J.M. Rodríguez-Izquierdo, M.A. Cauqui, Catalysis Today 154 (2010) 195.
[27] F. Arena, G. Trunfio, B. Fazio, J. Negro, L. Spadaro, Journal of Physical Chemistry C 113 (2009) 2822.